ELSEVIER

Nuclear Physics A 629 (1998) 621-634

NUCLEAR PHYSICS A

# Dipole band structures in $^{195}$Hg

N. Nenoff [a], G. Baldsiefen [a], H. Hübel [a], A. Görgen [a], W. Korten [a,1], M.A. Deleplanque [b], R.M. Diamond [b], P. Fallon [b], I.Y. Lee [b], A.O. Macchiavelli [b], F.S. Stephens [b]

[a] *Institut für Strahlen- und Kernphysik, Universität Bonn, Nussallee 14-16, D-53115 Bonn, Germany*

[b] *Lawrence Berkeley National Laboratory, Berkeley, CA 94720, USA*

Received 5 September 1997; revised 31 October 1997; accepted 25 November 1997

**Abstract**

High-spin states in $^{195}$Hg have been investigated using the GAMMASPHERE Ge-detector array in its early implementation phase. The level scheme has been extended up to an excitation energy of about 10 MeV and a spin of 71/2 $\hbar$. Three new dipole band structures have been added for which $B(\mathrm{M1}, \Delta I = 1)/B(\mathrm{E2}, \Delta I = 2)$ branching ratios were determined to be of the order of 2 $(\mu_n/\mathrm{eb})^2$. Possible quasiparticle excitations responsible for these structures are discussed.


*PACS:* 21.10.-k; 21.10.hw; 27.80.+w
*Keywords:* Nuclear reactions $^{192}$Os($^9$Be,6n); $E$ = 80 MeV; Measured $\gamma\gamma$-coin.; $E_\gamma$; DCO ratios; $^{195}$Hg deduced levels; Dipole bands; $J$; $\pi$; Compton-suppressed Ge detectors; BGO detectors

## 1. Introduction

A large number of band structures consisting of enhanced magnetic-dipole transitions and weak electric-quadrupole crossover transitions have been discovered in recent years in the Hg–Pb region [1]. While the bands with regular energy spacings in the Pb [2] and Bi [3] isotopes could be explained in terms of magnetic rotation [4], the interpretation of the dipole structures in the Hg isotopes [5–11] is not so clear. In the latter nuclei the dipole structures are less regular and probably not caused by magnetic rotation. Magnetic rotation should not be responsible for the observed dipole bands in the Hg isotopes because configurations with a large magnetic dipole moment perpendicular to

[1] Present address: DAPNIA, CEA Saclay, F-91191 Gif-sur-Yvette, France.

0375-9474/98/$19.00 
*PII* S0375-9474(98)00653-2

the spin that can cause magnetic rotation [4] lie at higher energy than in the Pb isotopes. The reason is that relatively low-energy $h_{11/2}$ proton excitations within the $Z = 82$ shell are possible. At oblate deformation these low-$K$ Nilsson orbitals can easily align along the rotation axis. Together with the low-$K$ $i_{13/2}$ neutron-hole orbitals they form high-spin excitations without a large transverse component of the magnetic moment. Such a component, as it appears in the Pb and Bi isotopes, is required for the occurrence of magnetic rotation [4].

In this work we report on an investigation of high-spin states in $^{195}$Hg. To date no dipole sequences have been reported in this nucleus. We find three such structures, extending the previously known level scheme [12] up to an excitation energy of about 10 MeV and a spin of 71/2 $\hbar$. In the following section the experimental procedure and the results will be presented. The level scheme and possible configurations for the magnetic-dipole bands will be discussed in the last section.

## 2. Experimental procedure and results

The experiment was performed at the Lawrence Berkeley National Laboratory 88-Inch Cyclotron. High-spin states in $^{195}$Hg were populated in the $^{192}$Os($^{9}$Be,6n) reaction at a beam energy of 80 MeV. The target consisted of a stack of three thin self-supporting foils with a total thickness of 0.99 mg/cm$^2$ of isotopically enriched $^{192}$Os (99%). Gamma-ray coincidences were measured using the GAMMASPHERE multi-detector array in its early implementation phase of 36 Compton-suppressed Ge detectors. The Ge detectors were placed at 17.3°, 31.7°, 37.4°, 90°, 142.6°, 148.3° and 162.7° to the beam axis. A total of $4 \times 10^8$ $\gamma$-ray coincidence events were collected on magnetic tapes. At our beam energy the main reaction products were $^{194}$Hg (64%) and $^{195}$Hg (22%), and $^{192}$Pt and $^{193}$Pt were also produced in $\alpha xn$ exit channels. High-spin states in $^{195}$Hg were also populated [13] with the $^{186}$W($^{18}$O,$\alpha$5n) reaction in an experiment at the Vivitron accelerator at Strasbourg, and $\gamma$-ray coincidences were measured with the Eurogam II array. These data were used to extract linear-polarization information on several crucial transitions.

In the off-line analysis the coincidences were unpacked into two- and three-fold events and sorted into $E_\gamma$-$E_\gamma$ matrices and into one $E_\gamma$-$E_\gamma$-$E_\gamma$ cube. In addition to the full $E_\gamma$-$E_\gamma$ matrix, two gated matrices were created with energy windows on several $\gamma$-ray transitions selecting specific decay paths. For the determination of the directional correlation (DCO) ratios similar matrices were sorted, but with the 90° detectors on one axis and the detectors at an average angle of 28.8° (151.2°) on the other axis. The DCO ratios were determined from coincidence spectra with gates on known stretched E2 transitions. The values were normalized to 1.0 for known E2 transitions; this gives DCO ratios around 0.5 for stretched dipole transitions. Our values are generally in agreement with previously known ratios [12] as far as they were available.

The $\gamma$-ray intensities were determined in the total projection spectrum of the full $E_\gamma$-$E_\gamma$ matrix for the strong uncontaminated transitions. For weaker transitions or unresolved

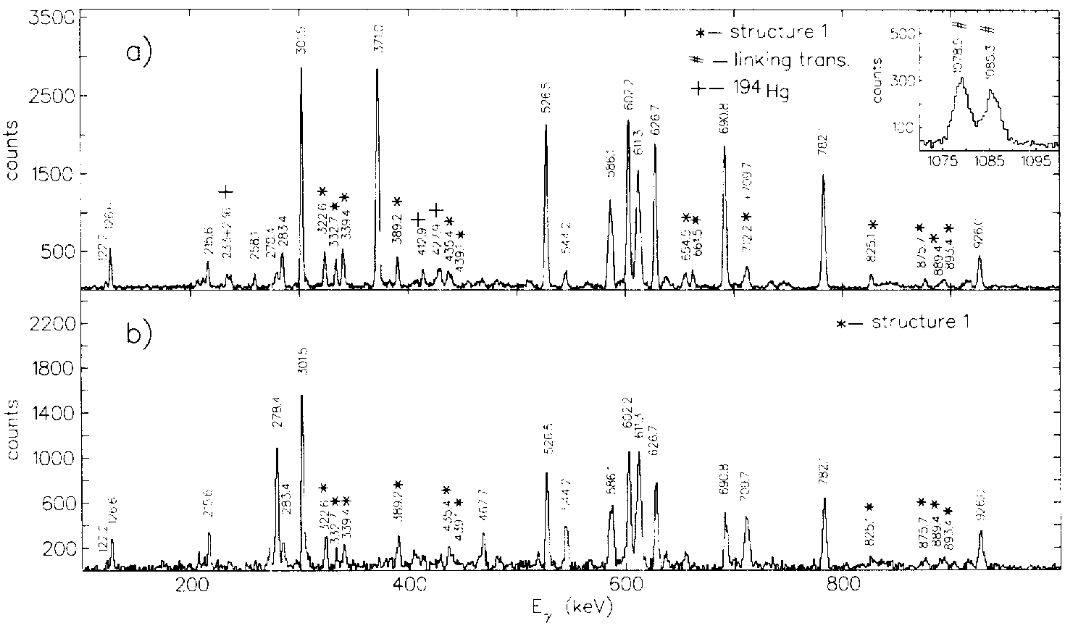


Fig. 1. Sum of triple-coincidence spectra showing transitions of structure 1 in $^{195}$Hg; (a) the first gate on the 926.0, 1078.5, or 1085.3 keV transition and the second gate on the 126.6, 526.5, 586.1, 690.8, or 782.1 keV transition; (b) the first gate on the 322.6, 332.7, 389.2, or 439.1 keV transition of structure 1 and the second gate on the 371.0 keV transition.

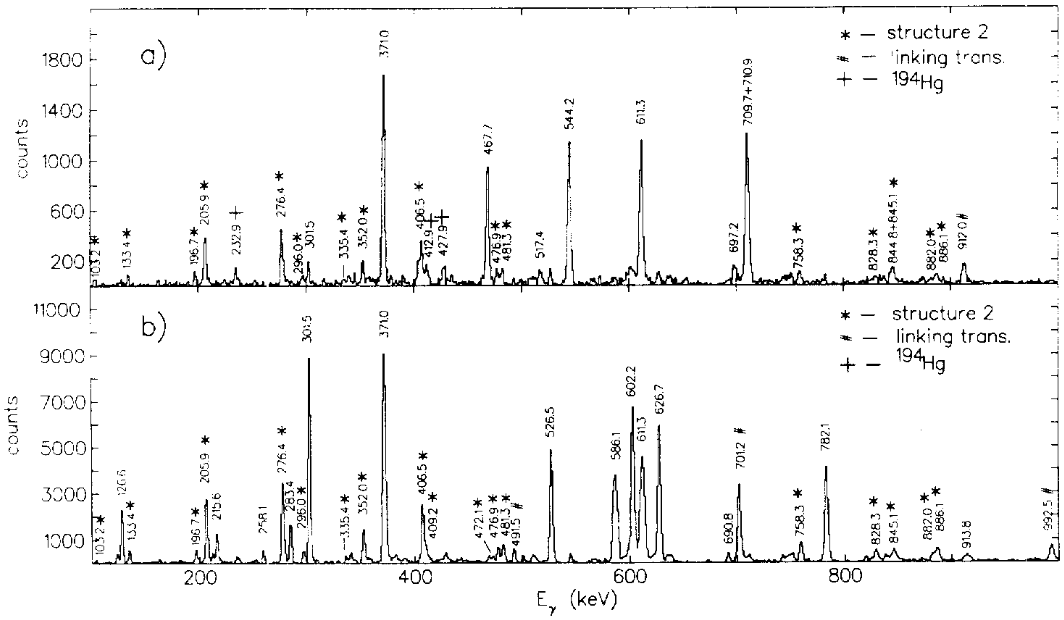


Fig. 2. Sum of triple-coincidence spectra showing transitions of structure 2 in $^{195}$Hg with the first gate on a transition of structure 2 and the second gate on: (a) the 278.4 keV transition (ABC band); (b) the 126.6, 526.5, 586.1, or 782.1 keV transition.

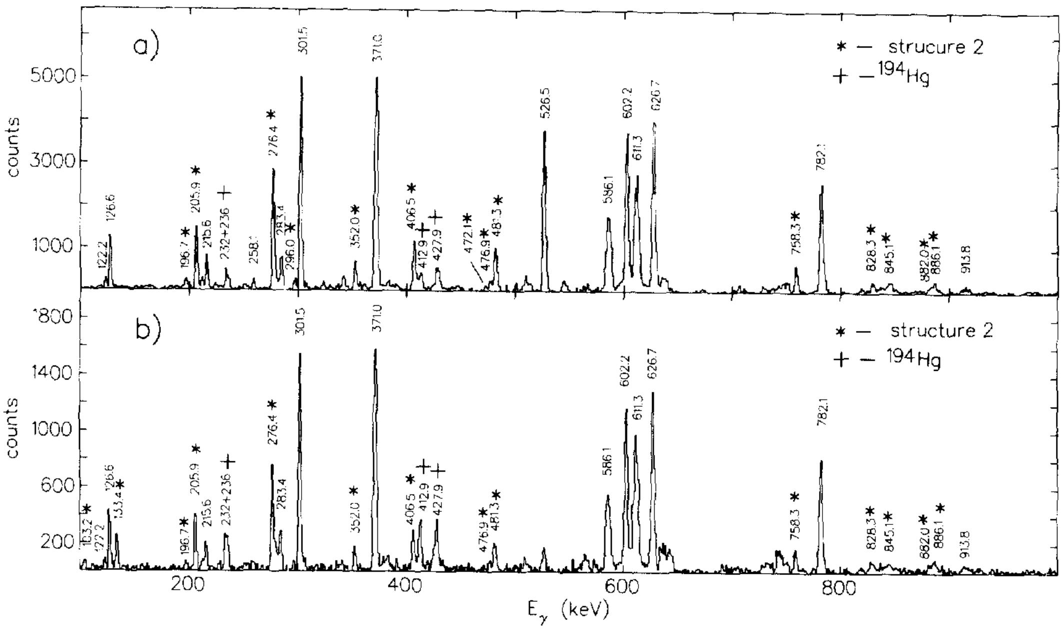


Fig. 3. Sum of triple-coincidence spectra showing transitions of structure 2 in $^{195}$Hg with the first gate on a transition of structure 2 and the second gate on: (a) the 701.2 keV transition; (b) the 992.5 keV linking transition.

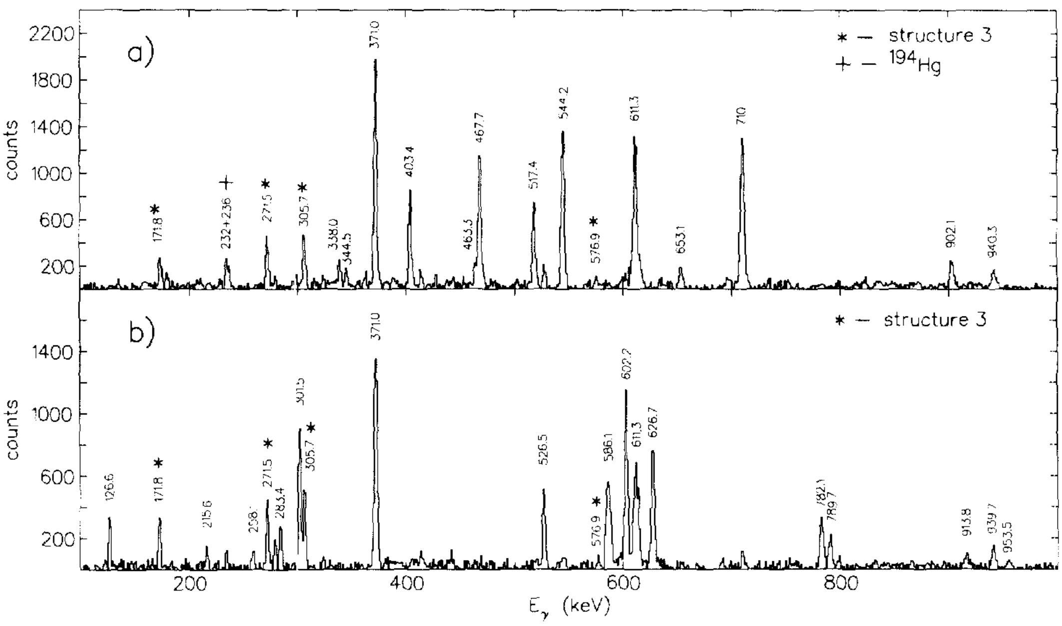


Fig. 4. Sum of triple-coincidence spectra showing transitions of structure 3 in $^{195}$Hg with the first gate on transitions of structure 3 and the second gate on: (a) the 278.4 keV transition (ABC band); (b) the 301.5, 526.5, or 782.1 keV transition.

Table 1
Transition energies, $\gamma$-ray intensities, DCO ratios, excitation energies and spin assignments of transitions in $^{195}Hg$

| Energy [a] | Intensity [b] | DCO | Excitation [e] | Assignment | | |
|---|---|---|---|---|---|---|
| $E_\gamma$ (keV) | $I_\gamma$ (rel.) | $I_\gamma(30°)/I_\gamma(90°)$ | $E_i$ (keV) | $I_i^\pi$ | → | $I_f^\pi$ |
| *General scheme* | | | | | | |
| 89.6 | 7 [d] | | 1996 | 29/2⁻ | → | 27/2⁻ |
| 122.2 | 25(4) | 0.47(7) | 1691 | 23/2⁻ | → | 21/2⁻ |
| 126.6 | 87(8) | 0.94(6) | 1695 | 25/2⁻ | → | 21/2⁻ |
| 174.0 [c] | 5(2) | | 4805 | 43/2⁺ | → | |
| 177.7 [c] | 4(2) | | above 3903 | | | |
| 211.2 | 24(4) | 0.91(15) | 1906 | 27/2⁻ | → | 25/2⁻ |
| 215.6 | 77(8) | 0.90(12) | 1906 | 27/2⁻ | → | 23/2⁻ |
| 258.1 | 18(3) | 0.48(6) | 1568 | 21/2⁻ | → | (19/2⁺) |
| 271.5 | 7(2) | | 5077 | | → | 43/2⁺ |
| 278.4 | 425(46) | 1.0(1) | 2515 | 33/2⁺ | → | 29/2⁺ |
| 283.4 | 68(6) | 0.53(5) | 1568 | 21/2⁻ | → | 19/2⁽⁺⁾ |
| 297.7 | 10(2) | 0.92(15) | 3386 | 37/2⁺ | → | 33/2⁽⁺⁾ |
| 301.5 | 352(29) | 1.07(9) | 1996 | 29/2⁻ | → | 25/2⁻ |
| 301.5 [c] | 4(2) | | 672 | | → | 17/2⁺ |
| 338.0 | 8(3) | 0.3(1) | 5415 | | | |
| 344.5 [c] | 2(1) | | 5421 | | | |
| 347.7 | 18(2) | 1.0(2) | 3386 | 37/2⁺ | → | 33/2⁺ |
| 356.7 | 12(3) | | above 4534 | | | |
| 361.6 | 8(2) | | 3690 | 39/2 | → | |
| 371.0 | 1000(50) | 1.0 | 371 | 17/2⁺ | → | 13/2⁺ |
| 381.5 | 12(4) | | above 1568 | | | |
| 403.4 | 93(8) | 1.02(7) | 3386 | 37/2⁺ | → | 37/2⁺ |
| 434.6 | 10(3) | | 3523 | 37/2⁺ | → | 33/2⁽⁺⁾ |
| 444.3 [c] | 3(1) | | 5077 | | | |
| 463.3 | 57(6) | 0.92(9) | 3690 | 39/2 | → | 35/2 |
| 467.7 | 324(28) | 1.02(8) | 2982 | 37/2⁺ | → | 33/2⁺ |
| 484.4 | 20(4) | 1.3(3) | 3523 | 37/2⁺ | → | 33/2⁺ |
| 491.5 [c] | 18(3) | 0.65(13) | 5717 | 51/2⁺ | → | 49/2⁻ |
| 517.4 | 99(8) | 1.05(8) | 3903 | 41/2⁺ | → | 37/2⁺ |
| 526.5 | 262(19) | 1.07(9) | 4534 | 45/2⁻ | → | 41/2⁻ |
| 544.2 | 508(39) | 1.1(1) | 2236 | 29/2⁺ | → | 25/2⁺ |
| 546.9 | 62(7) | 0.9(1) | 2453 | 31/2⁻ | → | 27/2⁻ |
| 555.7 [c] | 10(3) | | 4961 | | | |
| 573.9 | 26(4) | | 3088 | 33/2⁽⁺⁾ | → | 33/2⁺ |
| 576.8 | 7(2) | | 5205 | 47/2⁻ | → | 43/2⁻ |
| 586.1 | 460(45) | 1.1(1) | 1568 | 21/2⁻ | → | 21/2⁺ |
| 602.2 | 420(28) | 0.97(6) | 2599 | 33/2⁻ | → | 29/2⁻ |
| 605.4 | 20(3) | 0.96(8) [d] | 4628 | 43/2⁻ | → | 39/2⁻ |
| 611.3 | 1000(50) | 1.03(5) | 982 | 21/2⁺ | → | 17/2⁺ |
| 626.7 | 330(27) | 1.1(1) | 4007 | 41/2⁻ | → | 37/2⁻ |
| 638.1 | 15(3) | 0.28(8) | 1310 | (19/2⁺) | → | |
| 653.1 | 71(6) | 0.98(8) | 4343 | 43/2 | → | 39/2 |
| 663.1 | 14(4) | | 5625 | | | |
| 672.1 | | 0.46(20) [d] | 672 | | → | 13/2⁺ |
| 685.1 [c] | 5(2) | | 5998 | | | |

Table 1 — continued

| Energy [a] | Intensity [b] | DCO | Excitation [c] | Assignment | | |
|---|---|---|---|---|---|---|
| $E_\gamma$ (keV) | $I_\gamma$ (rel.) | $I_\gamma(30°)/I_\gamma(90°)$ | $E_i$ (keV) | $I_i^\pi$ | → | $I_f^\pi$ |
| 689.9 [c] | 6(2) | | 5415 | | → | $45/2^+$ |
| 690.8 | 113(14) | 1.08(9) | 5225 | $49/2^-$ | → | $45/2^-$ |
| 696.0 [c] | 8(2) | | 5421 | | → | $45/2^+$ |
| 697.2 | 38(6) | 0.90(15) | 4221 | $41/2^+$ | → | $37/2^+$ |
| 701.2 | 67(7) | 0.53(6) | 5235 | $47/2^+$ | → | $45/2^-$ |
| 707.6 | 65(10) | | 3690 | 39/2 | → | $37/2^+$ |
| 709.7 | 536(45) | 1.06(8) | 1692 | $25/2^+$ | → | $21/2^+$ |
| 710.9 | 102(15) | 0.8(3) | 3693 | $41/2^+$ | → | $37/2^+$ |
| 711.8 | 54(9) | 0.36(5) [d] | 3226 | 35/2 | → | $33/2^+$ |
| 729.5 [c] | 13(3) | 0.9(2) | 5998 | | | |
| 733.6 | 15(4) | 0.44(12) | 5077 | | → | 43/2 |
| 739.0 | 38(4) | 1.1(1) | 3192 | $35/2^-$ | → | $31/2^-$ |
| 751.2 | 7(2) | | above 5717 | | | |
| 782.1 | 354(24) | 1.1(1) | 3381 | $37/2^-$ | → | $33/2^-$ |
| 787.4 [c] | 13(4) | | above 2515 | | | |
| 789.7 [c] | 14(2) | 0.56(11) | 5324 | | → | $45/2^-$ |
| 801.8 | 35(5) | 0.71(12) | 3038 | $33/2^+$ | → | $29/2^+$ |
| 813.6 | 13(3) | 0.3(1) | 3328 | | → | $33/2^+$ |
| 821.2 | 37(5) | 0.92(9) | 4724 | $45/2^+$ | → | $41/2^+$ |
| 830.3 | 23(3) | 1.1(1) | 4022 | $39/2^-$ | → | $35/2^-$ |
| 833.4 | 12(3) | 0.88(13) | above 2982 | | | |
| 840.4 | 10(3) | | above 2982 | | | |
| 844.8 | 30(5) | 0.52(12) | 5066 | | | |
| 851.2 | 11(3) | | 3088 | $33/2^{(+)}$ | → | $29/2^+$ |
| 872.9 | 48(5) | 1.1(1) | 4566 | $45/2^+$ | → | $41/2^+$ |
| 890.1 | 17 [d] | 1.3(2) [d] | 2582 | $(29/2^+)$ | → | $25/2^+$ |
| 902.1 | 44(5) | 0.52(7) | 4805 | $43/2^+$ | → | $41/2^+$ |
| 912.0 [c] | 32(5) | 0.82(15) | 5133 | $45/2^+$ | → | $41/2^+$ |
| 913.8 | 69(11) | 0.36(4) [d] | 1286 | $19/2^{(+)}$ | → | $17/2^+$ |
| 926.0 | 67(7) | 1.1(1) | 6151 | $53/2^-$ | → | $49/2^-$ |
| 926.2 | 27(5) | 0.9(2) | 5269 | | → | 43/2 |
| 939.7 | 22(4) | 0.47(8) [d] | 1310 | $(19/2^+)$ | → | $17/2^+$ |
| 940.3 [c] | 6(2) | | above 4805 | | | |
| 942.0 | 11(3) | | 4632 | | → | 39/2 |
| 953.5 | 12(4) | | 4961 | | → | $41/2^-$ |
| 967.5 [c] | 4(2) | | 5692 | | → | $45/2^+$ |
| 970.2 [c] | 17(3) | 0.9(2) | 5313 | | → | 43/2 |
| 992.5 | 28(4) | 0.52(7) | 5000 | $43/2^+$ | → | $41/2^-$ |
| 1006.9 | 15(4) | 1.3(3) | 5573 | $49/2^+$ | → | $45/2^+$ |
| 1013.4 [c] | 6(2) | | 7012 | | | |
| 1024.8 | 6(2) | 0.60(14) | 4406 | | → | $37/2^-$ |
| 1061.4 [c] | 9(3) | 1.3(3) | 5786 | | → | $45/2^+$ |
| 1078.5 [c] | 29(4) | 1.0(2) | 7229 | $57/2^-$ | → | $53/2^-$ |
| 1085.3 [c] | 26(4) | 1.2(2) | 7236 | $57/2^-$ | → | $53/2^-$ |
| 1239.2 [c] | 18(4) | 0.8(2) | 4221 | $41/2^+$ | → | $37/2^+$ |
| 1307.3 [c] | 5(3) | | 5000 | $43/2^+$ | → | $41/2^+$ |
| 1440.9 [c] | 10(2) | | 5133 | $45/2^+$ | → | $41/2^+$ |
| 1603.5 [c] | 10(3) | | above 982 | | | |

Table 1 — continued

| Energy [a] | Intensity [b] | DCO | Excitation [e] | Assignment | | |
|---|---|---|---|---|---|---|
| $E_\gamma$ (keV) | $I_\gamma$ (rel.) | $I_\gamma(30°)/I_\gamma(90°)$ | $E_i$ (keV) | $I_i^\pi$ | → | $I_f^\pi$ |
| *Structure 1* | | | | | | |
| 322.6 [c] | 19(3) | 0.46(9) | 7891 | $61/2^-$ | → | $59/2^-$ |
| 332.7 [c] | 14(3) | 0.36(9) | 7569 | $59/2^-$ | → | $57/2^-$ |
| 339.4 [c] | 20(4) | 0.43(8) | 7569 | $59/2^-$ | → | $57/2^-$ |
| 389.2 [c] | 19(4) | 0.33(9) | 8280 | $63/2^-$ | → | $61/2^-$ |
| 435.4 [c] | 11(3) | 0.30(12) | 8716 | $65/2^-$ | → | $63/2^-$ |
| 439.1 [c] | 6(2) | | 9155 | $67/2^-$ | → | $65/2^-$ |
| 454.0 [c] | 5(2) | | 9609 | $69/2^-$ | → | $67/2^-$ |
| 654.5 [c] | 13(3) | 1.1(2) | 7891 | $61/2^-$ | → | $57/2^-$ |
| 661.5 [c] | 16(4) | 1.0(2) | 7891 | $61/2^-$ | → | $57/2^-$ |
| 712.2 [c] | 17(6) | 1.2(3) | 8280 | $63/2^-$ | → | $59/2^-$ |
| 825.1 [c] | 17(3) | 0.65(20) | 8716 | $65/2^-$ | → | $61/2^-$ |
| 875.7 [c] | 12(3) | 0.67(22) | 9155 | $67/2^-$ | → | $63/2^-$ |
| 889.4 [c] | 6(2) | | 10045 | $71/2^-$ | → | $67/2^-$ |
| 893.4 [c] | 12(3) | | 9609 | $69/2^-$ | → | $65/2^-$ |
| *Structure 2* | | | | | | |
| 103.2 [c] | 6(2) | | 5235 | $47/2^+$ | → | $45/2^+$ |
| 133.4 [c] | 14(3) | 0.46(9) | 5133 | $45/2^+$ | → | $43/2^+$ |
| 196.7 [c] | 9(3) | 0.43(8) | 6320 | 55/2 | → | $53/2^+$ |
| 205.9 | 48(5) | 0.43(8) | 5717 | $51/2^+$ | → | $49/2^+$ |
| 276.4 | 84(11) | 0.45(6) | 5512 | $49/2^+$ | → | $47/2^+$ |
| 296.0 [c] | 9(3) | 0.42(11) | 6616 | 57/2 | → | 55/2 |
| 335.4 [c] | 8(3) | | 6952 | $57/2^+$ | → | 57/2 |
| 352.0 [c] | 31(4) | 0.38(8) | 6475 | $55/2^+$ | → | $53/2^+$ |
| (378.6) [c] | 9(3) | | 5512 | $49/2^+$ | → | $45/2^+$ |
| 406.5 | 48(5) | 0.39(8) | 6123 | $53/2^+$ | → | $51/2^+$ |
| 409.2 [c] | 7(2) | 0.65(15) | 7362 | $59/2^+$ | → | $57/2^+$ |
| 472.1 [c] | 5(2) | | 7834 | $61/2^+$ | → | $59/2^+$ |
| 476.9 [c] | 18(3) | 0.35(6) | 6952 | $57/2^+$ | → | $55/2^+$ |
| 481.3 | 40(4) | 1.0(1) | 5717 | $51/2^+$ | → | $47/2^+$ |
| 611.5 [c] | 25(6) | | 6123 | $53/2^+$ | → | $49/2^+$ |
| 758.3 [c] | 41(5) | 0.90(8) | 6475 | $55/2^+$ | → | $51/2^+$ |
| 828.3 [c] | 22(4) | 1.5(3) | 6952 | $57/2^+$ | → | $53/2^+$ |
| 845.1 [c] | 16(5) | 0.87(15) | 8207 | $63/2^+$ | → | $59/2^+$ |
| 882.0 [c] | 12(3) | | 7834 | $61/2^+$ | → | $57/2^+$ |
| 886.1 [c] | 19(4) | | 7362 | $59/2^+$ | → | $55/2^+$ |
| *Structure 3* | | | | | | |
| 171.8 [c] | 16(3) | 0.55(7) | | | | |
| 271.5 | 32(5) | 0.42(6) | | | | |
| 305.7 | 31(5) | 0.42(5) | | | | |
| 576.9 [c] | 9(3) | | | | | |

[a] Uncertainties between 0.1 and 0.8 keV, depending on intensity.
[b] Relative intensities normalized to the 371 keV transition.
[c] Gamma-ray transition observed for the first time in this work.
[d] Adopted from Ref. [12].
[e] Uncertainties between 0.2 and 1.0 keV.

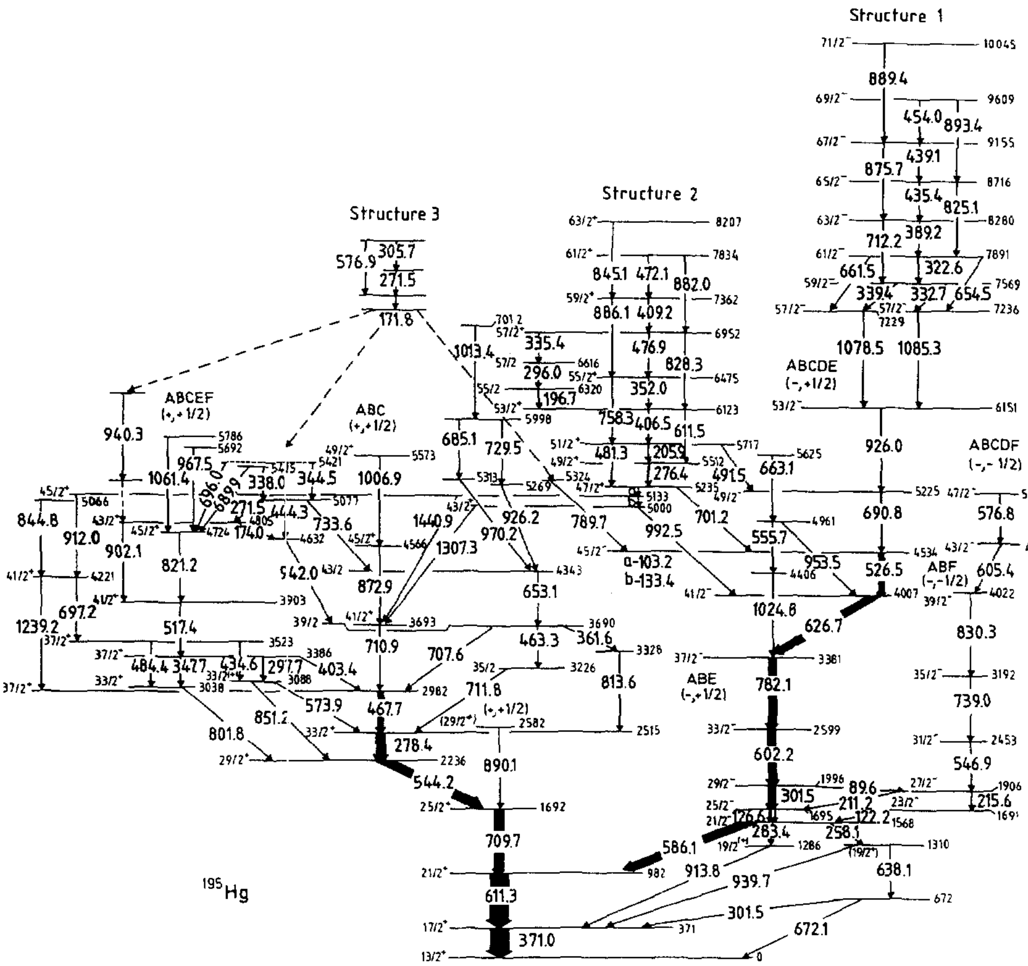


Fig. 5. Level scheme of $^{195}$Hg.

lines they were determined in single- or double-gated coincidence spectra and properly normalized. The experimental $\gamma$-ray energies, intensities and DCO ratios as well as the assignments in the level scheme are summarized in Table 1. Figs. 1–4 show examples of the $\gamma$-ray coincidence spectra which were chosen mainly to give evidence for the three new dipole structures established in our work. The spectrum in Fig. 1a was created from a matrix obtained with gates on transitions of the ABCDE band; the others were obtained from a three-dimensional $\gamma$-$\gamma$-$\gamma$ cube which was limited in energy to 1 MeV. In the spectra with gates on transitions of the ABE and ABCDE bands the 371.0, 586.1, and 611.3 keV lines show Doppler broadening, probably due to a lifetime of the 1568 keV state.

The energy-level scheme of $^{195}$Hg based on our data is displayed in Fig. 5. In the lower- and medium-spin part and for the strongly populated states it is in agreement with the previous work of Mehta et al. [12]. We have observed about 60 new $\gamma$-ray transitions and nearly all of them have been placed in the level scheme. A total of 32 new levels have been added to the previously known scheme, extending it up to about

10 MeV and a spin of 71/2 $\hbar$. The majority of the transitions that were previously assigned to $^{195}$Hg but could not be placed in the level scheme [12] are now established, except for the 202.6, 232.8, 252.4, 303.0, 373.4, and 748.4 keV transitions which are partly contaminated by strong $\gamma$-ray lines of similar energies in neighbouring $^{194}$Hg. The previously identified level at 2582 keV could not be confirmed unambiguously in our work because the 890.1 keV $\gamma$-ray depopulating this level lies close to lines of similar energy in the high-spin part of the scheme. The 5421 keV level has been placed tentatively in the level scheme and is shown as a dashed line because the position of the 344.5 keV transition is uncertain. A possible alternative might be that this transition is the highest member of structure 3.

In the following we will not comment on each new level but rather concentrate on the three new sequences of enhanced dipole transitions which are labelled "Structure 1, 2 and 3" in Fig. 5. They consist of $\Delta I = 1$ dipole, presumably M1, transitions and $\Delta I = 2$ E2 crossover transitions. Structures 1 and 2 are firmly connected to the lower-spin states, but structure 3, which is weaker and consists of only four levels, could not be linked to the other states. Its main decay paths are indicated by the three dashed lines shown in the level scheme.

Structure 1 is built on top of the previously known strongly populated band with negative parity and decays via two stretched-quadrupole transitions of 1078.5 and 1085.3 keV. The linear polarization of these transitions is compatible with E2 multipolarity, but the statistical accuracy is rather poor. Structure 1 has therefore most probably also negative parity. The most strongly populated state of 7891 keV collects about 5% of the intensity of the 371 keV level. Gamma-ray coincidence spectra showing the transitions of structure 1 and its decay are displayed in Fig. 1. About 70% of the decay goes into the negative-parity band mainly via the 1078.5 and 1085.3 keV transitions. The remaining 30% decay branch to the positive-parity yrast sequence remains unobserved.

Gamma-ray coincidence spectra showing the transitions of structure 2 and its decay are displayed in Figs. 2 and 3. The M1 multipolarity could only be established for the 352.0 and 406.5 keV transitions by the linear-polarization analysis. The three levels, with energies of 5235, 5512, and 5717 keV, were already placed by Mehta et al. [12]. We extend this sequence up to 8.2 MeV. The level with the strongest population is the 5717 keV state which collects about 15% of the intensity of the 371 keV level. Structure-2 decays with about equal intensity to the positive- and negative-parity yrast states, but about 30% of the decay intensity has not been observed. Of the three transitions with energies of 491.5, 701.2, and 992.5 keV linking structure 2 with the negative-parity yrast band, the 701.2 keV transition has the highest intensity. For this transition, which has the DCO ratio of a stretched dipole, the linear polarization shows that it is an E1 transition. This determines positive parity for structure 2.

Structure 3 consists only of four transitions; the 271.5 and 305.7 keV transitions were already observed in the previous work [12]. Our data show a complicated decay path, the main intensity flow going into the positive-parity levels (about 70%). Because the decay is highly fragmented it was not possible to link structure 3 to the lower-lying states.

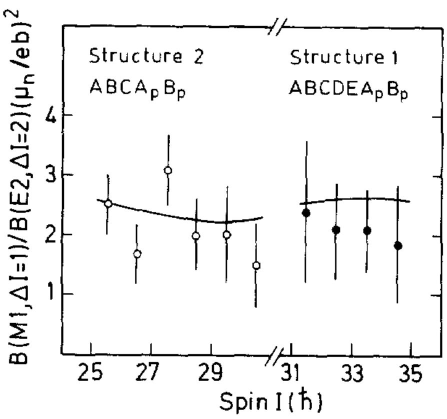


Fig. 6. Experimental and calculated $B(\mathrm{M1})/B(\mathrm{E2})$ ratios. The experimental alignment, $K = 2$ and $Q = -2.7$ b were used in the calculation, see text.

Recently, superdeformation was found in $^{195}$Hg [14], populated in the reaction $^{150}$Nd($^{48}$Ca,3n). We do not find these superdeformed bands in our data, but we see, very weakly, the superdeformed yrast band in $^{194}$Hg. Note that the reaction channel leading to $^{194}$Hg has about three times the intensity compared to the $^{195}$Hg channel. Furthermore, probably superdeformed states are populated with less intensity in the $^{9}$Be-induced reaction used in this experiment.

## 3. Discussion

The low- and medium-energy parts of the level scheme shown in Fig. 5 consist predominantly of cascades of stretched E2 transitions. Similar band structures have also been observed in the neighbouring Hg isotopes. Cranked shell model (CSM) [15] calculations have shown that these structures are bands built on different weakly oblate neutron quasi-particle excitations that are crossing each other with rather small interaction energies [16]. We have adopted (and included in Fig. 5 to label the bands) the CSM classification of the various quasi-particle excitations. The letters A, B, C, ... denote unnatural-parity quasi-neutrons (of $i_{13/2}$ origin) with increasing excitation energy, while E, F, ... are the lowest-energy natural-parity quasi-neutrons.

The new sequences of levels with spin difference $\Delta I = 1$ have a very different structure. Similar bands have recently also been observed at high spin and excitation energy in several neighbouring Hg isotopes [5-11]. In most cases they could not be connected to the lower-energy part of the level scheme. Here, in $^{195}$Hg, structures 1 and 2 are firmly linked to the lower levels and their spins and excitation energies are well established. The weaker structure 3 is not connected and we do not want to speculate on the possible configuration that might be responsible for this excitation.

If we assume that the $\Delta I = 1$ transitions are pure M1, we can deduce the $B(\mathrm{M1}, \Delta I = 1)/B(\mathrm{E2}, \Delta I = 2)$ ratios from the measured intensity branching ratios. The ratios, which are shown in Fig. 6, lie around 2 $(\mu_n/\mathrm{eb})^2$. They are rather similar to the ones found in the neighbouring Hg isotopes [5-11], but they are about an order of magnitude

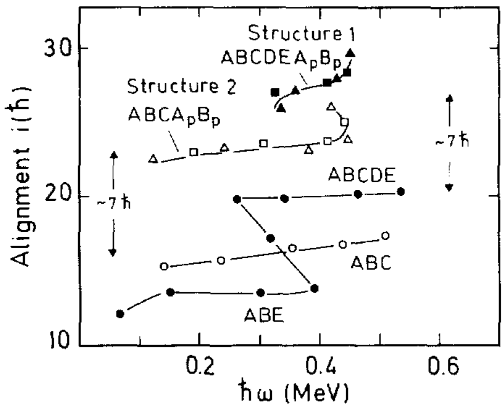


Fig. 7. Experimental aligned angular momenta for the different bands in $^{195}$Hg as a function of rotational frequency. The reference-core parameters $J_0 = 8\ \hbar^2/\mathrm{MeV}$ and $J_1 = 40\ \hbar^4/\mathrm{MeV}^3$ were used [6].

smaller than the ones observed in the "shears bands" of the Pb isotopes [2,17,18]. The shears bands are built on proton-particle excitations across the $Z = 82$ shell gap into the high-$K$ $h_{9/2}$ and $i_{13/2}$ orbitals that are coupled to low-$K$ $i_{13/2}^{-n}$ neutron–hole states [2]. The lowest energy of such a particle–hole coupling is obtained for a perpendicular orientation of the proton- and neutron-spin vectors. This coupling gives rise to a large component of the magnetic moment, $\mu_\perp$, perpendicular to the total angular momentum. Since this component of the magnetic moment is responsible for the dipole radiation, the M1 transitions are strongly enhanced and the $B(\mathrm{M1})/B(\mathrm{E2})$ ratios lie around 20–40 $(\mu_n/\mathrm{eb})^2$ for the shears bands in the Pb isotopes.

The smaller $B(\mathrm{M1})/B(\mathrm{E2})$ ratios in the Hg isotopes probably result from smaller $B(\mathrm{M1})$ values because it is unlikely that the $B(\mathrm{E2})$ values are an order of magnitude larger than the ones in the Pb isotopes. Somewhat larger $B(\mathrm{E2})$ values may be expected because the quadrupole deformation, at least at low spin, is larger in the Hg isotopes compared to that of the Pb nuclei [18–20]. On the other hand, total routhian surface calculations show [19] that the deformation decreases drastically if the the proton $s_{1/2}$ orbital, which is empty at low excitation energy in the Hg isotopes, is occupied, e.g. by the proton $h_{11/2}$ – $s_{1/2}$ excitation.

The smaller $B(\mathrm{M1})$ values reflect the fact that other proton excitations and different couplings are involved in the Hg isotopes. Because of the closed $Z = 82$ shell, proton excitations in the Pb isotopes can only take place across the shell gap. On the oblate side it takes little energy to excite protons into the $h_{9/2}$ and $i_{13/2}$ orbitals. The lowest-energy Nilsson orbitals have high-$K$ and are not easy to align. For the Hg isotopes, however, there are two holes in the proton shell. This allows proton excitations within the shell which, depending on the deformation, may cost less energy. Low-$K$ $h_{11/2}$ hole states which align easily and other low-j orbitals may be populated. Such configurations do not result in large $\mu_\perp$ components and, hence, the $B(\mathrm{M1})$ values are expected to be smaller than those for the shears bands in the Pb isotopes, which always involve the proton $h_{9/2}$ and $i_{13/2}$ orbitals coupled with a large angle to neutron $i_{13/2}$ hole excitations.

Structure 1 has negative parity because it decays to the ABCDE configuration via stretched E2 transitions (see Fig. 5). The experimental alignment, which is shown in Fig. 7, is about 27 $\hbar$ and lies approximately 7 $\hbar$ above that of the ABCDE band. It is most likely that a $h_{11/2}$ proton pair ($A_pB_p$) is responsible for this additional alignment. The maximum alignment gain from this pair of protons would be 10 $\hbar$, but the data suggest that they are not fully aligned. This occurs frequently in this mass region. For example, in the neighbouring odd–odd Au isotopes bands based on the not completely stretched $(\nu i_{13/2} \otimes \pi h_{11/2})_{11}$ states are known [21,22]. Such a non-stretched coupling, which was also suggested for a $\Delta I = 1$ band in $^{192}$Hg [19], can explain the observed alignment and the $B$(M1) values.

In Fig. 6 the experimental $B(\mathrm{M1})/B(\mathrm{E2})$ ratios are compared to calculations. For structure 1 we assume the $ABCDEA_pB_p$ configuration as just discussed and use the Dönau–Frauendorf formula [23] to estimate the $B$(M1) values. A calculation, assuming $K = 2$, is shown. The $B$(E2) values were obtained using the quadrupole moments derived by Willsau et al. [19] for $^{192}$Hg.

A further argument for the configuration assignment comes from a comparison of experimental excitations to Hartree–Fock plus BCS calculations [7,24,25]. Indeed, two-proton-multi-neutron quasi-particle excitations are expected theoretically in the energy range around 8 MeV. The calculations seem to overestimate the excitation energies by about 2 MeV, but one has to keep in mind that they were done for $^{192}$Hg and do not include particle-number projection and residual interactions between valence quasi-particles.

Structure 2 has positive parity. It decays with about equal intensity to the ABE and ABC configuration. As can be seen in Fig. 7, it shows an alignment of 24 $\hbar$ and the alignment gain with respect to the ABC quasi-neutron configuration is about 7 $\hbar$. This is the same alignment gain as found for structure 1. The $B(\mathrm{M1})/B(\mathrm{E2})$ ratios are also similar for the two structures. Thus, the same arguments can be made for the partial alignment of a $h_{11/2}$ proton pair, which in this case would be coupled to the ABC configuration. The same Hartree–Fock calculations also predict such excitations in the right energy range of about 6 MeV.

## 4. Summary

In summary, high-spin states in $^{195}$Hg have been populated in the $^{192}$Os($^{9}$Be, 6n) reaction and high-fold $\gamma$-ray coincidences have been measured using the GAMMASPHERE Ge-detector array. The level scheme has been extended to considerably higher spins and excitation energies. Three new $\Delta I = 1$ structures were found, two of which have been connected to the lower-lying levels. On the basis of their excitation energies, $B(\mathrm{M1})/B(\mathrm{E2})$ ratios and alignments the quasi-particle configurations $ABCDEA_pB_p$ and $ABCA_pB_p$ are suggested for structures 1 and 2, respectively.

## Acknowledgements

We are indebted to the authors of Ref. [13] for allowing us to use their data for the linear-polarization analysis. The work was supported by DOE under contract DE-AC03-76SF00098, by NATO grant CRG 930496 and by DFG and BMBF, Germany.

## References


[1] R.B. Firestone, Table of Isotopes, ed. V.S. Shirley, C.M. Baglin, S.Y.F. Chu and J. Zipkin (Wiley, 1996).

[2] G. Baldsiefen, H. Hübel, W. Korten, U.J. van Severen, J.A. Cizewski, N.H. Medina, D.R. Napoli, C. Rossi Alvarez, G. Lo Bianco and S. Signorelli, Z. Phys. A 355 (1996) 337 and references therein

[3] P.J. Dagnall, C.W. Beausang, R.M. Clark, R. Wadsworth, S. Bhattacharjee, P. Fallon, P.D. Forsyth, D.B. Fossan, G. deFrance, S.J. Galet, F. Hannachi, K. Hauschild, I.M. Hibbert, H. Hübel, P.M. Jones, M.J. Joyce, A. Korichi, W. Korten, D.R. LaFosse, E.S. Paul, H. Schnare, K. Starosta, J.F. Sharpey-Schafer, P.J. Twin, P. Vaska, M.P. Waring and J.N. Wilson, J. Phys. G 20 (1994) 1591, and references therein.

[4] S. Frauendorf, Conf. on Nucl. Structure Around the Turn of the Century, Crete (1996) and Z. Phys. A, in press.

[5] N. Roy, J.A. Becker, E.A. Henry, M.J. Brinkman, M.A. Stoyer, J.A. Cizewski, R.M. Diamond, M.A. Deleplanque, F.S. Stephens, C.W. Beausang and J.E. Draper, Phys. Rev. C 47 (1993) R930.

[6] B. Cederwall, M.-A. Deleplanque, F. Azaiez, R.M. Diamond, P. Fallon, W. Korten, I.-Y. Lee, A.O. Macchiavelli, J.R.B. Oliveira, F.S. Stephens,W.H. Kelly, D.T. Vo, J.A. Becker, M.J. Brinkman, E.A. Henry, J.R. Hughes, A. Kuhnert, M.A. Stoyer, T.F. Wang, J.E. Draper, C. Duyar, E. Rubel and J. deBoer, Phys. Rev. C 47 (1993) R2443.

[7] Y. Le Coz, N. Redon, A. Astier, R. Béraud, R. Duffait, M. Meyer, F. Hannachi, G. Bastin, I. Deloncle, B. Gall, M. Kaci, M.G. Porquet, C. Schück, F. Azaiez, C. Bourgeois, J. Duprat, A. Korichi, N. Perrin, N. Poffé, H. Sergolle J.F. Sharpey-Schafer, C.W. Beausang, S.J. Gale, M.J. Joyce, E.S. Paul, R.M. Clark, K. Hauschild, R. Wadsworth, J. Simpson, M.A. Bentley, A.G. Smith, H. Hübel, P. Willsau, G. De France, I. Ahmad, M. Carpenter, R. Henry, R.V.F. Janssens, T.L. Khoo and T. Lauritsen, Z. Phys. A 348 (1994) 87.

[8] D. Ye, K.B. Beard, U. Garg, R.V.F. Janssens, M.P. Carpenter, I. Ahmad, T.L. Khoo, E.F. Moore, F.L.H. Wolfs, Ph. Benet, Z.W. Grabowski and M.W. Drigert, Nucl. Phys. A 537 (1992) 207

[9] J.K. Deng, W.C. Ma, J.H. Hamilton, J.D. Garrett, C. Baktash, D.M. Cullen, N.R. Johnson, I.Y. Lee, F.K. McGowan, S. Pilotte, C.H. Yu and W. Nazarewicz, Phys. Lett. B 319 (1993) 63.

[10] N. Fotiades, S. Harissopulos, C.A. Kalfas, S. Kossionides, C.T. Papadopoulos, R. Vlastou, M. Serris, M. Meyer, N. Redon, R. Duffait, Y. Le Coz, L. Ducroux, F. Hannachi, I. Deloncle, B. Gall, M.G. Porquet, C. Schuck, F. Azaiez, J. Duprat, A. Korichi, J.F. Sharpey-Schafer, M.J. Joyce, C.W. Beausang, P.J. Dagnall, P.D. Forsyth, S.J. Gale, P.M. Jones, E.S. Paul, J. Simpson, R.M. Clark, K. Hauschild and R. Wadsworth, J. Phys. G 21 (1995) 991.

[11] N. Fotiades, S. Harissopulos, C.A. Kalfas, S. Kossionides, C.T. Papadopoulos, R. Vlastou, M. Serris, J.F. Sharpey-Schafer, M. J. Joyce, C.W. Beausang, P.J. Dagnall, P.D. Forsyth, S.J. Gale, P.M. Jones, E.S. Paul, P.J. Twin, J. Simpson, D.M. Cullen, P. Fallon, M.A. Riley, R.M. Clark, K. Hauschild and R. Wadsworth, Z. Phys. A 354 (1996) 169.

[12] D. Mehta, Y.K. Agarwal, K.P. Blume, S. Heppner, H. Hübel, M. Murzel, K. Theine, W. Gast, G. Hebbinghaus, R.M. Lieder and W. Urban, Z. Phys. A 339 (1991) 317.

[13] I.M. Hibbert, R. Wadsworth, K. Hauschild, H. Hübel, W. Korten, U.J. van Severen, E.S. Paul, A.N. Wilson, J.N. Wilson, A.P. Byrne, W. Satuła and R. Wyss, Phys. Rev. C 54 (1996) 2253.

[14] G. Hackman, R. Krücken, R.V.F. Janssens, M.A. Deleplanque, M.P. Carpenter, D. Ackermann, I. Ahmad, H. Amro, S. Asztalos, D.J. Blumenthal, R.M. Clark, R.M. Diamond, P. Fallon, S.M. Fischer, B. Herskind, T.L. Khoo, T. Lauritsen, I.-Y. Lee, R.W. MacLeod, A.O. Macchiavelli, D. Nisius, G.J. Schmid, F.S. Stephens, K. Vetter and R. Wyss, Phys. Rev. C 55 (1997) 148.

[15] R. Bengtsson and S. Frauendorf, Nucl. Phys. A 327 (1979) 139.

[16] H. Hübel, A.P. Byrne S. Ogaza, A.E. Stuchbery, G.D. Dracoulis and M. Guttormsen, Nucl. Phys. A 453 (1986) 316.

[17] M. Neffgen, G. Baldsiefen, S. Frauendorf, H. Grawe, J. Heese, H. Hübel, H. Kluge, A. Korichi, W. Korten, K.H. Maier, D. Metha, J. Meng, N. Nenoff, M. Piiparinen, M. Schönhofer, R. Schubart, U.J. van Severen, N. Singh, G. Sletten, B.V. Thirumala Rao and P. Willsau, Nucl. Phys. A 595 (1995) 499.

[18] R.M. Clark, S.J. Asztalos, G. Baldsiefen, J.A. Becker, L. Bernstein, M.A. Deleplanque, R.M. Diamond, P. Fallon, I.M. Hibbert, H. Hübel, R. Krücken, I.Y. Lee, A.O. Macchiavelli, R.W. MacLeod, G. Schmid, F.S. Stephens, K. Vetter, R. Wadsworth and S. Frauendorf, Phys. Rev. Lett. 78 (1997) 1868.

[19] P. Willsau, M. Neffgen, Y. Le Coz, H. Hübel, W. Korten, F. Hannachi, A. Korichi, M.G. Porquet, M. Kaci, N. Redon, M. Meyer, C.W. Beausang, E.S. Paul, J. Simpson and J.R. Hughes, Z. Phys. A 355 (1996) 129.

[20] C. Günther, H. Hübel, A. Kleinrahm, R. Kulessa, H. Emling, P. Fuchs, E. Grosse, D. Schwalm, H.J. Wollersheim, J. Idzko and H. Ower, Z. Phys. A 301 (1981) 119.
[21] A. Neskakis, R.M. Lieder, H. Beuscher, Y. Gono, D.R. Haenni, M. Müller-Veggian, Nucl. Phys. A 390 (1982) 53
[22] V.P. Janzen, Z.-M. Liu. M.P. Carpenter, L.H. Courtney, H.-Q. Jin, A.J. Larabee, L.L. Riedinger, J.K. Johansson, D.G. Popescu, J.C. Waddington, S. Monaro, S. Pilotte and F. Dönau, Phys. Rev. C 45 (1992) 613.
[23] F. Dönau, Nucl. Phys. A 471 (1987) 469.
[24] P. Bonche, S.J. Krieger, P. Quentin, M.S. Weiss, J. Meyer, M. Meyer, N. Redon, H. Flocard and P.-H. Heenen, Nucl. Phys. A 500 (1989) 308.
[25] M. Meyer, N. Redon, P. Quentin and J. Libert, Phys. Rev. C 45 (1992) 233.